



AUTHOR(S):

TITLE:

YEAR:

Publisher citation:

OpenAIR citation:

Publisher copyright statement:

This is the _____ version of proceedings originally published by _____
and presented at _____
(ISBN _____; eISBN _____; ISSN _____).

OpenAIR takedown statement:

Section 6 of the "Repository policy for OpenAIR @ RGU" (available from <http://www.rgu.ac.uk/staff-and-current-students/library/library-policies/repository-policies>) provides guidance on the criteria under which RGU will consider withdrawing material from OpenAIR. If you believe that this item is subject to any of these criteria, or for any other reason should not be held on OpenAIR, then please contact openair-help@rgu.ac.uk with the details of the item and the nature of your complaint.

This publication is distributed under a CC _____ license.

Tensile failure analysis of structural materials using acoustic emission

John .J. MOWAT ¹, Sha. JIHAN ¹, Mohamad .G. DROUBI ^{1,*}

¹ School of Engineering, Robert Gordon University, Aberdeen, AB10 7GJ, UK

*Corresponding author, E-mail: m.g.droubi@rgu.ac.uk

Abstract

Materials' testing is an extremely important process in the modern world with new colossal structures being built in every corner of the earth, with the ever-increasing size of structures making safety of vital importance. This research therefore aims to characterise the failure behaviour of three commonly used structural metals, namely Steel, Aluminium and Brass, when subjected to tensile loading. The tensile load was applied to each of the metallic specimen at four different loading rates whilst using the Acoustic Emission (AE) technique as a monitoring tool to record elastic waves produced from the materials until failure. Fractography was also examined in this study to correlate the AE signals with microscopic deformation characteristics of the materials. The AE activity was superimposed on the loading graph for each material tested. The graph was divided into three distinct regions (elastic, plastic and failure) and the recorded AE was compared. All three materials displayed a unique intensity of acoustic emission. The results showed that for the three materials, steel produced the most amount of AE activity for all loading rates tested. It was also observed that the highest accumulation of AE activity concentrated at the elastic region. The AE signals were found to be amplified when increasing the displacement rate of tensile load applied to specimens. Each material displayed unique characteristics in relation to the AE activity with defining features when monitoring until failure. The AE technique proved effective at distinguishing between the three materials, when applied with a tensile load until failure. Therefore, the proposed AE monitoring technique can be useful to effectively monitor failure characteristics and to assess the overall structural health of such materials to ensure their integrity.

Keywords: Acoustic Emission, Tensile testing, Structural material, Failure analysis, Fractography.

1. INTRODUCTION

Tensile testing of materials has been conducted for many years, dating all the way back to Galileo Galilei (1564-1642) [1], where more recent innovations in the field have enabled development of specialised equipment to improve the accuracy of the testing. The drive to enhance the knowledge and understanding of material failure is highly regarded, with the concepts of reliability and safety increasingly becoming priority throughout industry. The knowledge of the failure characteristics of structural materials is of high importance in industrial applications, as unexpected failures can cause breakdown and plant shutdown causing companies extensive loss in revenue.

Acoustic Emission (AE) technique is a Non-destructive testing (NDT) method that uses the transient elastic waves produced when a material undergoes stress/deformation as a result of an external force, and can be recorded using transducers to reveal the size, shape and possible position of the waves if multiple sensors are implemented. In 1953, Joseph Kaiser performed

the first documented results using an AE technique, discovering what is referred to as ‘*Kaiser Effect*’ [2]. Since then, use of the technique has caused a surplus of further work to be conducted in more recent years. The applicability of the AE technique has been measured against numerous testing methods, including low speed rotational machinery, where predication of loose and fractured bolts was verified [3]. Many studies have looked into different AE characteristics regarding various tensile tests. Testing concerning mild steel specimens subjected to central and off-centre holes produced results insinuating the two largest AE signals occur in succession before failure, with the voided specimens creating AE signals earlier than that of perfect specimens [4]. A similar investigation using stainless steel specimens supported this claim with the use of notches opposed to holes, with greater AE activity contrasting to the perfect specimens [5]. Looking into the mechanical behaviour of the material, Marsudi concluded that the AE activity was visibly denser within the elastic region of the failure, with the AE signals seemingly dropping linearly till final failure, though a fairly recent investigation has opposing claims that no visible AE signals are displayed prior to yield point when using aluminium specimens [6-7].

The use of ‘*Fractography*’ as an investigation technique has been seen to enable verification of fracture types when using AE as a monitoring technique [6], with further analysis to be made regarding the mechanisms of failure in different materials.

The entire research is focused on the use of AE technique to monitor and examine the AE characteristics of different tensely loaded metallic materials at varying loading rates. These materials are widely used in structural applications where identifying the material deformation under load is paramount for safety and recognition of the onset of failures. Therefore, the objective of this work is to investigate the failure characteristics of two commonly used structural materials (steel and aluminium) when subjected to tensile loading, where brass was included for comparison.

2. EXPERIMENTAL PROCEDURES

The experimental work was carried out using identically dimensioned ‘dog-bone’ specimens, as shown in Figure 1. Each specimen was dimensioned to the EN 10002-1:2001 standards, and manufactured from long length bar and milled accordingly to ensure accurate measurements and prevention of heat distortion. The dog-bone specimens allow relative control of the fracture position, where the fracture will occur through the smaller cross-section.

An Instron 1195 tensile testing machine was used to apply the tensile load to the individual specimens, with a full-scale load cell range set to 50kN. The crosshead displacement rate was varied through the different tests: 0.05 mm/min, 0.1 mm/min, 0.2 mm/min and 0.5mm/min. The specified load ranges for the tests were set by calculating the estimated tensile force to fail each type of specimen. The average Ultimate Tensile Strength (UTS) of the material was acquired in order to obtain the maximum tensile force required to fail each specimen (Table 1). Using a Vernier caliper, the dimensions of the smaller section were measured and the cross sectional area (A), which was assumed constant for all specimens, was then determined to give $4.03225 \times 10^{-5} m^2$. Equation 1 forms the resultant force required to fail the specimen, where the maximum load range was set consequently on the Instron tensile testing machine.

$$F = A \times \sigma \quad (1)$$

| Material | Steel | Aluminium | Brass |
|------------------------|-------|-----------|-------|
| UTS, σ (MPa) | 340 | 550 | 410 |

Table 1: Ultimate tensile strength of investigated materials

AE monitoring was performed in all cases using an AMSY 4 system, produced by Vallen. The signals produced were recorded by two 20 mm diameter Duncagan SE150-M high performance AE sensors, with a 100-300 kHz frequency range. The sensors were placed at both wide end locations of the dog-bone specimen (See Figure 2), within the grip length and spacing defined in Figure 1. Both sensors were mounted to the specimen and RS 494-124 Silicone grease was applied to prevent air interference between the surface of sensor and specimen. Multiple sensor mounting techniques were explored and tested, and optimum contact pressure and reduction of slippage was created using binding clips.

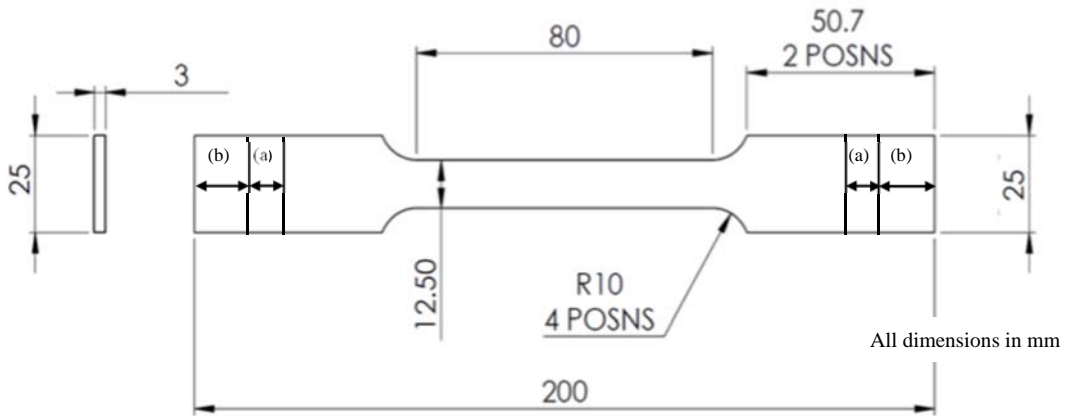


Figure 1: Specimen dimensions and configuration (a) Spacing = 10 mm; (b) Grip length = 20 mm

The Vallen AMSY4 system and the Instron 1195 were linked directly using the parametric input (see Figure 2); this enabled simultaneous recording of AE activity against load data in real-time. A sampling rate of 0.625 MHz/s with a 35.5dB threshold was set for all tests. Data was analysed through the Visual AE application within the VALLEN software, where different AE parameters could be plotted against each other for investigation.

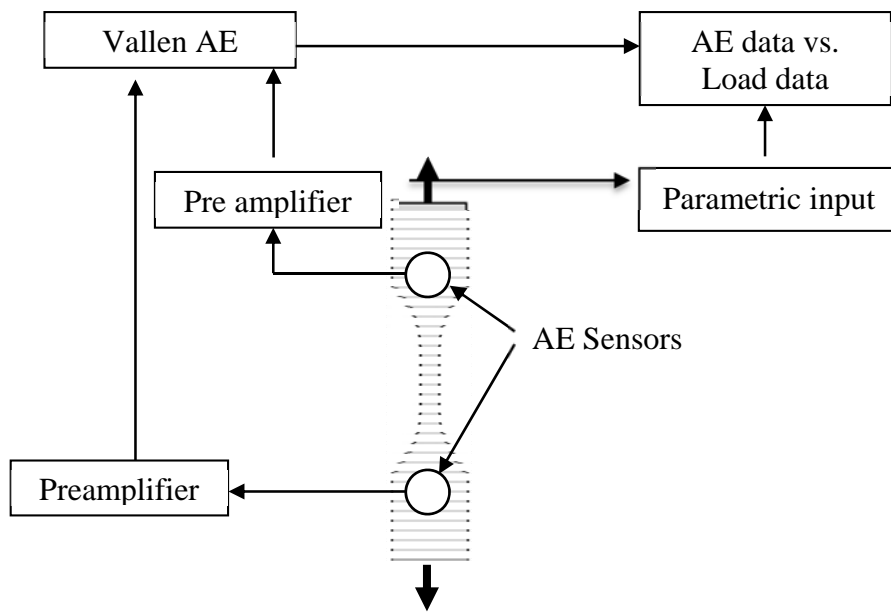


Figure 2: Schematic of experimental set-up

4. RESULTS AND DISCUSSION

4.1 Interpretation Method

To quantify the results, the employed method by Chuluunbat et al. [7], was implemented. This method as illustrated in Figure 3, involved dividing the loading/time graphs into three definitive regions (R1, R2, and R3), and discussing the AE results within these sections respectively.

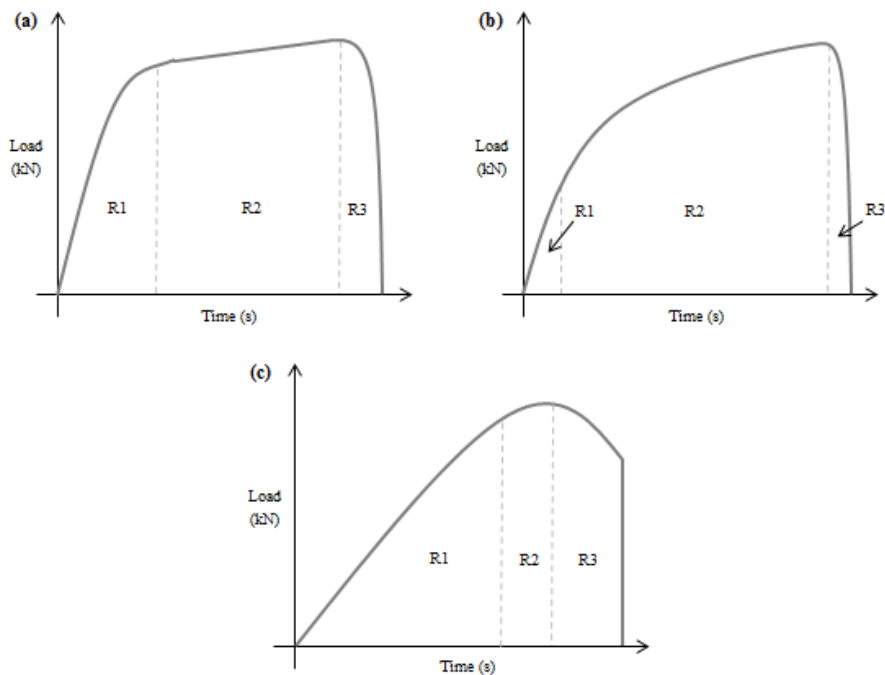


Figure 3: Metallic tensile loading regions (a) aluminium; (b) brass; (c) steel

Variations in physical properties within the three different materials produce uniquely shaped loading/time graph for each material, depicting three similar regions. In [Figure 3](#), it is shown that region 'R1' begins at the initial tensile loading, up to the upper yield of material, where the stress increases linearly with increasing load. Region 'R2' begins at the end of region 'R1', and ends at the UTS of the material, where the applied load reaches its limit. Region 'R3' begins at the end of region 'R2', and ends where the material succumb to ultimate failure, and the resultant load graph drops to 'zero' as there is no longer any resistance to the applied displacement.

4.2 Analysis of Acoustic Emission

4.2.1 Steel

Comparing all three different materials on initial observations reveal AE monitoring to be most sensitive for steel specimens (see [Figure 4a](#)). Individual regions reveal to be recognisable through AE analysis with region R1 proving to be **'noiser'** (*higher rate of AE accumulation*) than following regions, in agreement with Muhammad Marsudi's [\[6\]](#) findings where AE activity for mild steel was denser in the elastic zone (region R1). The first half of region R1 was particularly denser with clear distinction of the junctions between the regions. Region R1 for the steel specimens dominated the majority of the overall testing time as a result of the materials high tensile strength. At the initial stage of loading (for all loading rates tested), a single pulse of AE activity was produced with amplitude readings between 37-45dB. Similar amplitude readings were recorded for all material combinations around the same time of load application. This leads to believe that the signals were produced from grip tightening and not due to material deformation, where the Instron jaw applies a 'gripping' force with exerted tensile load.

AE activity in region R2 was observed to be minimal. All tests produced single pulse signals when reaching region R2, signifying when material was close to the UTS. At loading rate 0.1 mm/min, the amplitude of particular pulse signals ranged between 55-60dB, this was almost identical when subjecting the specimen to 0.05 mm/min displacement rate. However, when increasing the displacement rate further to 0.2 mm/min and 0.5 mm/min, it was realised the same distinctive traits were realised relating to the respective load graphs and signal amplitudes, however, the density of AE signals was considerably enhanced. In almost all tests, AE activity was recognisable at the onset of failure, where high density pulse signals occurred around 90-95dB. Differentiating between particular values at this point in pursuit of determining relationships would be impractical, as material had already failed at this point.

4.2.2 Aluminium

Analysis of the aluminium AE plots revealed AE activity in region R1 to be denser than the following two regions, at all loading rates tested. Initial significant amplitude signals ranging between 53-70dB for a displacement rate of 0.1 mm/min was observed at the mid-point of region R1, where there was an extremely minimal gradient change towards the horizontal axis, but continuing to increase rapidly due to strain hardening. The stretching of bonds at this point within the elastic region is 'self-reversing' [\[9\]](#) and will return to its original shape if the applied tensile force is removed, as atoms are not yet slipping past each other. Amplitude of signals at the displacement rate of 0.05 mm/min was suitably lower, where 34dB was recorded, but still producing clear signal distinction in conjunction with loading graphs. The signal density for the specimen tested at a 0.5 mm/min displacement rate was found to be enlarged

throughout the test, indicating that the increased displacement rate had an amplified effect on the density of the AE signals. The greatest density of the signals was observed at the end of the region R1 at the yeild point (see Figure 4b) of the material where the loading graph direction drastically sloped towards the horizontal. Signal amplitude at this point was reasonably noticable ranging between 50-65dB for majority of the experiments conducted.

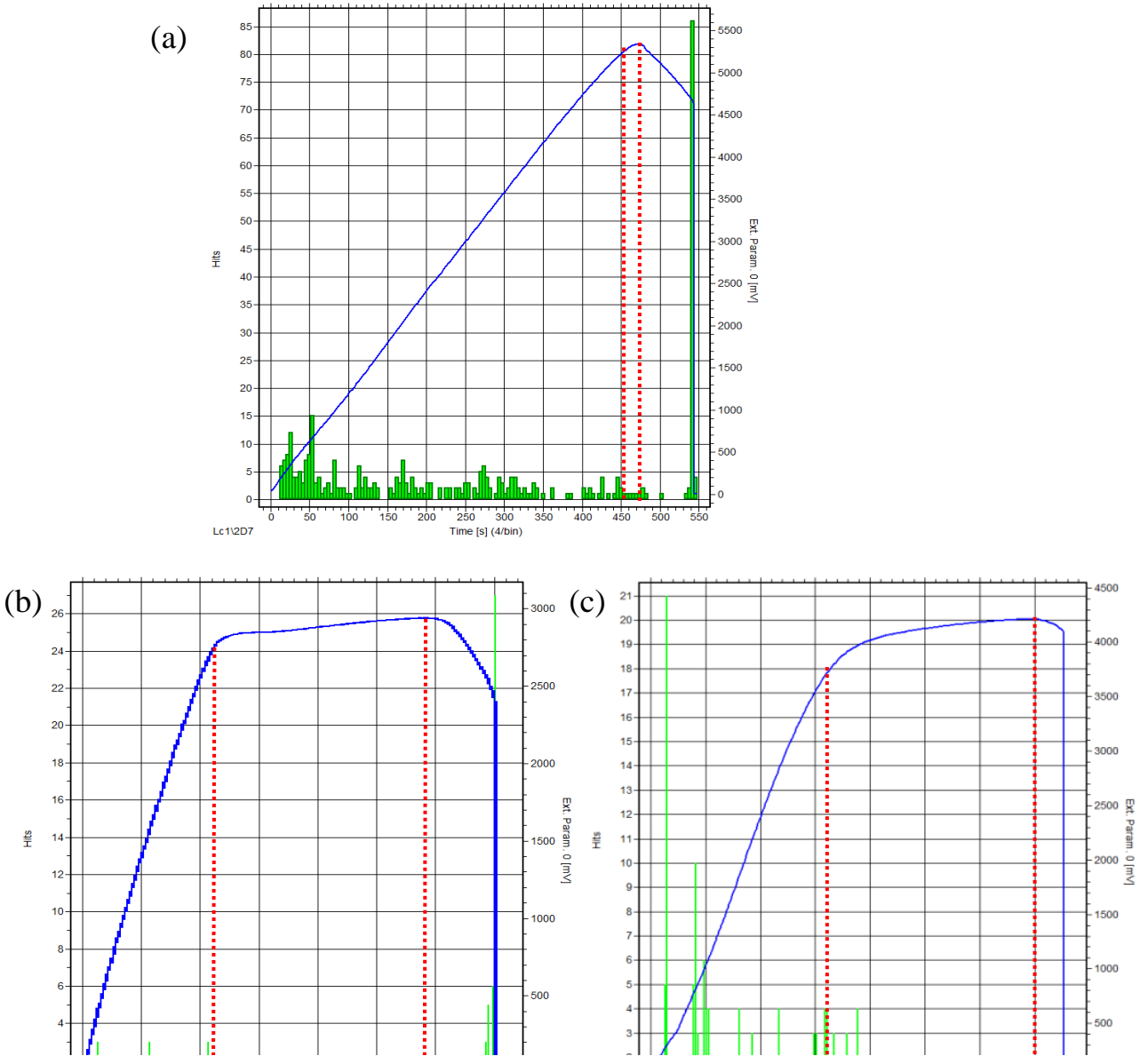


Figure 4: Stress and cumulative counts/hits versus time for displacement rate = 0.1 mm/min; (a) steel, (b) aluminium, and (c) brass

After the yeild point, the stress created by loading is adequate to deform permanently. The individual AE hits/counts was caused by breaking of atomic bonds by movement of dislocations [8], explaining the quantity of individual AE hits observed. Hit density continued to show dominance throughout the entire yeild point for all displacement rates tested. The remainder of region R2 for all loading rates for aluminium was visually '**quieter**' (*lower rate*

of AE accumulation) than region R1. The end of region R1/beginning of region R2 was easy to differentiate due to the high hit density throughout the yield point occurrence. It can be seen in Figure 4c that strain hardening also occurs after the material yield in region R2, where the material cross-section has begun to reduce and ‘necking’ [8] has started to occur.

At the end of region R2, obvious signals in pulse form were observed for all displacement rates tested. Specimens tested at 0.5 mm/min produced corresponding results although the density decreased at lower displacement rates. At the UTS of the material, the gradient on the graph was no longer increasing; at this point ‘necking’ was visibly evident (See Figure 5). The high elasticity of aluminium allowed further deformation than the other two material types. AE in region R3 through this occurrence was insignificant till final failure.

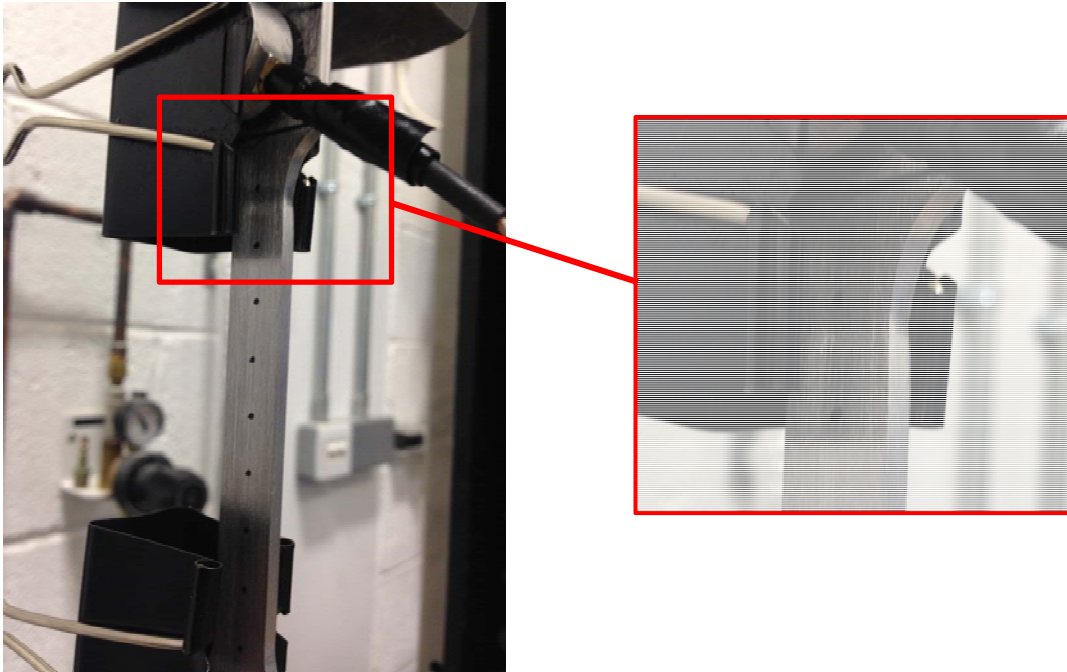


Figure 5: Necking observed on aluminium specimen during tensile testing

4.2.3 Brass

Similar to both steel and aluminium, brass exhibited much denser AE activity in region R1 in comparison to the other two regions. Brass in contrast produced extremely miniscule sum of AE signals beyond yield point, and nil in most cases. The highest signal density recorded was at the halfway point of the region at about 50 seconds for the specimen tested at 0.2 mm/min. When increasing speed further to 0.5 mm/min similar characteristics was evident however, the end of the region produced extremely high-density AE signals. This indicated when yield point was reached, and hence the high-density AE signals correlated to that phenomenon. The end of the region was extremely recognisable due to the sudden disappearance of the AE activity, even more drastic than that of the aluminium test specimens, especially when increasing displacement rate to 0.2 mm/min and 0.5 mm/min. Region R3 for all Brass specimens was undistinguishable due to absence of AE activity. This may be a good resource to use for predicting onset of failure in brass components.

4.2.4 Investigation of fracture microstructure

The steel specimens were observed to have ‘tensile tearing’ present, shown by the river lines or stress lines, these lines always converge in the direction of local crack propagation. The type of fracture associated with the above characteristics is called a **transgranular cleavage fracture** [8]. [Figure 6a](#) shows very small ‘microvoids’ present on the surface of the fracture around the particles. Due to the excessive amount of microvoids on the surface of steel opposed to the other two materials, it was believed that the high density AE activity was produced from microvoid formation.

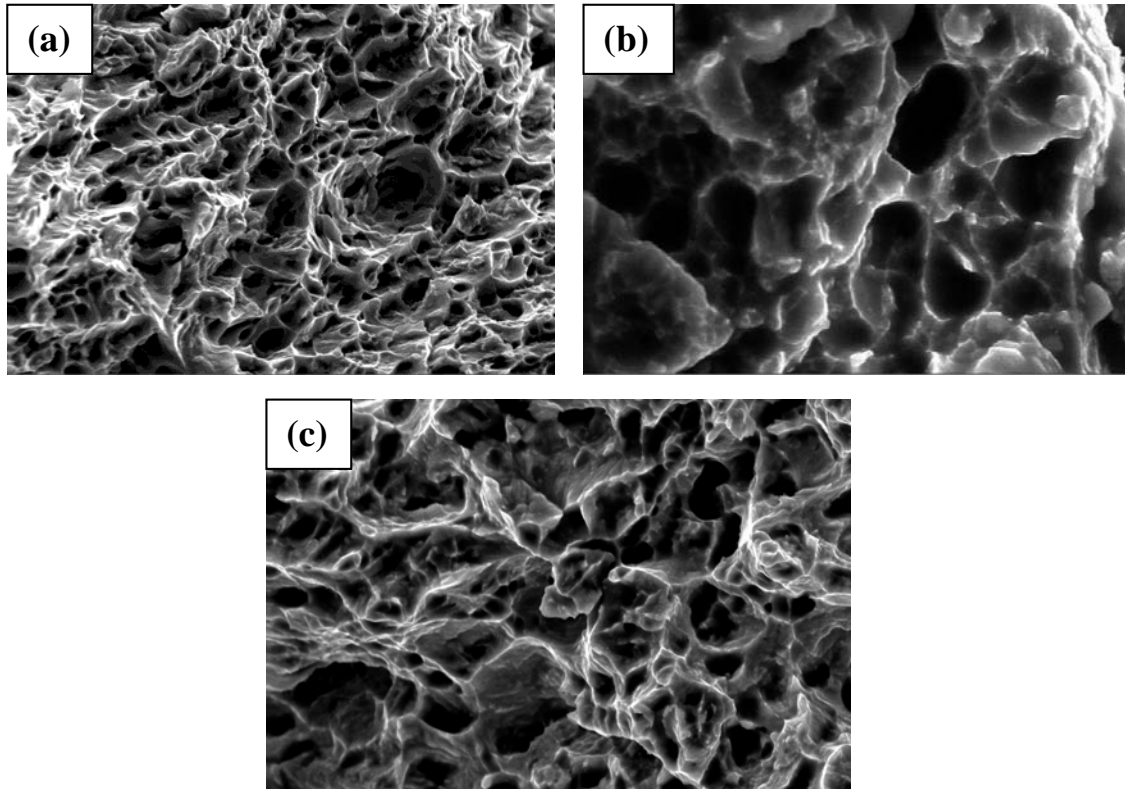


Figure 6: SEM photographs of specimen fracture surface at 5000x magnification (a) steel; (b) aluminium; (c) brass

The initial observation of the SEM photographs of aluminium specimens indicated a ductile fracture through the depth of the microvoids as shown in [Figure 6b](#); the deeper the microvoids the higher the material ductility. It however was known before SEM pictures were acquired that the aluminium specimens produced a ductile fracture as obvious necking was observed during tests ([Figure 5](#)). The distinctive AE signals at the yield point towards the end of region R1 indicate that the ductile fracture produced reasonable AE activity when the material moved into plastic deformation, where this could be identified as the most vital distinction of material phases for integrity monitoring.

Brass (see [Figure 6c](#)) showed a classic form of a brittle fracture. Indications of a brittle fracture are present where no traces of deformation were found on the grain boundaries. The microvoids present on the surface are very small and sharp. The brittle nature of the brass material could explain the lack of AE activity towards the failure, as the failure occurred extremely fast. The majority of AE data was experienced at the beginning where the bonds were stretching. Due to the brittle nature of the material, the failure will happen almost instantly after UTS is reached. A good indication on when to replace a component made of brass would be when AE

activity is no longer present. The absence of AE activity reveals the bonds are stretched to their limits where the bonds are ready to slip past each other and break.

5. CONCLUSIONS

Acoustic emission has been used to provide a better insight into the tensile behaviour of three common structural materials, namely steel, aluminium and brass. AE hits plots showed steel to be more sensitive in respect to AE activity recorded which was due to its microstructure as fractographic images of fracture surface reveal steel to have a much higher density of microvoids present. These microvoids were suspected to be the main cause of AE activity being released. AE activities for all steel specimens were observed to be denser in region R1, with first half of region R1 even more dominant than the second. All steel specimens created the first recognisable density of signals extremely early followed successively by the densest zone of signals, before drastically becoming quieter. This was attributed to the bonds beginning to stretch after suitable load is present.

Brass shows miniscule AE activity after end of region R1, with the resulting failure occurring very rapidly. When monitoring brass for structural integrity, a clear alarm as to when the component is about to fail is the lack of AE activity opposed to excessive distinctive activity.

Aluminium specimens produce very little AE activity in region R3 however; small signals were present when material had reached its UTS. At this point necking was visible where AE activity occurred due to extreme deformation of material through high ductility. High-density signals were observed through yield point of the material's bonds beginning to move past each other. The high-density signals at the yield point would indicate when to review the integrity of the component, as it signifies when the material is shifting into plastic deformation.

The increase in loading rate for all three metals increases AE activity throughout the entire test, highlighting various AE characteristics in the loading graphs more visibly. It was found that **ALL** materials exhibit much higher density signals in region R1 where the material is still within its suitable working range before the yield point. Region R1 indicates when the bonds of the material are being stretched, but no bonds are broken. A lack of AE activity when monitoring proved to be a more useful alarm when predicting the onset of failure of steel, aluminium and brass; rather than any outstanding AE signals. Relative monitoring of the accumulative AE signals created from tensely loaded components could prove a vital monitoring technique that could efficiently reduce sudden failure initiation in stressed materials and structures.

ACKNOWLEDGEMENTS

Authors are grateful for the Institute of Mechanical Engineers IMechE and the Robert Gordon University in providing a travel grant for conference attendance and presentation.

REFERENCES

- [1] Oveday MS, Gray T, Aegerter J. Tensile Testing of Metallic Materials: A Review. 2004; 1:8.
- [2] Grosse CU, Ohtsu M. History and Fundamentals. Acoustic Emissions Testing. Leipzig: Springer-Verlag Berlin Heidelberg; 2008. 2 p. 14.
- [3] Mba D. Applicability of Acoustic Emissions to Monitoring the Mechanical Integrity of Bolted Structures in Low Speed Rotating Machinery: Case Study. 2001

- [4] Singh SK, Srinivasan K, Chakraborty D. Acoustic Emission Studies on Metallic Specimen Under Tensile Loading. 2003
- [5] Mukhopadhyay CK, Ray KK, Jayakumar T, Raj B. Acoustic Emission from Tensile Deformation of Unnotched and Notched Specimens of AISI Type 304 Stainless Steels. 2007
- [6] Marsudi M. Study of Acoustic Emission During Tensile Test of Mild Steel Plate. 2011
- [7] Chuluunbat T, Lu C, Kostryzhev A, Tieu AK. Influence on Loading Conditions During Tensile Testing on Acoustic Emission. 2015
- [8] Móser M. Fractography with the SEM (Failure Analysis).
- [9] NDT Resource Centre. *Elastic/Plastic Deformation*. [homepage on the Internet]. NDT Resource Centre; 2014 cited 2016 23rd April]. Available from: <https://www.ndeed.org/EducationResources/CommunityCollege/Materials/Structure/deformation.htm>.